HHS Public Access

Author manuscript

*Science*. Author manuscript; available in PMC 2015 November 04.

Published in final edited form as:

*Science*. 2015 September 25; 349(6255): 1532–1536. doi:10.1126/science.aac8555.

# O–H hydrogen bonding promotes H-atom transfer from a C–H bonds for C-alkylation of alcohols

**Jenna L. Jeffrey**[*], **Jack A. Terrett**[*], and **David W. C. MacMillan**[†]

Merck Center for Catalysis, Princeton University, Princeton, NJ 08544, USA

## Abstract

The efficiency and selectivity of hydrogen atom transfer from organic molecules are often difficult to control in the presence of multiple potential hydrogen atom donors and acceptors. Here, we describe the mechanistic evaluation of a mode of catalytic activation that accomplishes the highly selective photoredox α-alkylation/lactonization of alcohols with methyl acrylate via a hydrogen atom transfer mechanism. Our studies indicate a particular role of tetra-*n*-butylammonium phosphate in enhancing the selectivity for α C–H bonds in alcohols in the presence of allylic, benzylic, α-C=O, and α-ether C–H bonds.

Complex molecules, such as medicinal agents and natural products, often possess multiple types of C–H bonds, each with a different inherent reactivity. This intrinsic reactivity depends on a multifaceted interplay of steric effects, inductive and conjugative influences, as well as innate strain (1, 2). The intermolecular catalytic functionalization of C($sp^3$)–H bonds in a selective manner represents a long-standing challenge that has inspired decades of effort within the synthetic community. Notable early studies by Bergman (3), as well as recent advances in selective intermolecular transition metal catalyzed C($sp^3$)–H activation—including, among others, Hartwig's rhodium-catalyzed borylation of terminal methyl groups (4) and White's iron-catalyzed oxidation of both secondary (2°) and tertiary (3°) aliphatic C–H bonds (5)—highlight the importance of catalyst structure on site selectivity.

Catalyst structure has also proven critical to the selectivity of C($sp^3$)–Hfunctionalization via hydrogen atom transfer (HAT) catalysis. HAT—the effective movement of a hydrogen atom between two molecular sites—represents a ubiquitous elementary reaction step in organic chemistry (6–8). The rate of hydrogen abstraction from a C–H bond depends not only on the C–H bond dissociation enthalpy (BDE) but also on polar effects in the transition state. In 1987, Roberts noted that certain electrophilic radicals (such as *t*-butoxyl) preferentially abstract hydrogen from electron-rich C–H bonds, whereas nucleophilic radicals (such as

[†]Corresponding author. dmacmill@princeton.edu.

[*]These authors contributed equally to this work.

**SUPPLEMENTARY MATERIALS**

www.sciencemag.org/content/349/6255/1532/suppl/DC1

Materials and Methods

Supplementary Text

References (*46–83*)

Data

DFT Calculations

amine-boryl) selectively cleave electron-deficient C–H bonds (9). The generality of this concept was subsequently delineated through the broad application of polarity reversal catalysis (PRC), which takes advantage of favorable polar effects to control the regioselectivity of HAT from multiple C–H groups of similar strength (10).

We questioned whether the basic principles of PRC could be integrated into a catalytic system for the selective activation of alcohol α-C–Hbonds in the presence of a wide range of other C–H bonds (such as α-C=O, α-ether, or allylic or benzylic C–H) (11, 12). Specifically, we postulated that the selective C-alkylation of alcohols could be achieved via a photoredox-catalyzed, H-bond–assisted bond activation strategy (Fig. 1) (13–15), in which the hydroxyalkyl C–H bond is selectively polarized and weakened via O–H hydrogen bonding.

It is well known that the strength of α C–H bonds of alcohols decreases upon deprotonation of the alcohol O–H group. This so-called “oxy anionic substituent effect” (16, 17) leads to the acceleration of a wide range of organic reactions [such as oxyanionic [1,3] and [3,3] sigmatropic rearrangements and HAT from alkoxides (18)]. More recently, it has been shown that intermolecular hydrogen bonding between alcohols and various acceptor molecules gives rise to a similar polarization and weakening of the adjacent C–H bond (19), the strength of which is reflected in the $^{13}C$ nuclear magnetic resonance (NMR) chemical shift and the one-bond $^{13}C$–$^{1}H$ coupling constant ($^{1}J_{CH}$) (20, 21). In particular, it was found that a 1 kJ/mol increase in the enthalpy of the H-bond resulted in a 0.2-Hz decrease in $^{1}J_{CH}$ for hexafluoroisopropanol complexed to various amines (20). On the basis of these studies, we reasoned that the efficiency and selectivity of alcohol C–H activation could be enhanced by catalytic complexation with a suitable hydrogen-bond acceptor. In particular, interaction of the hydroxyl group of an alcohol with a hydrogen-bond acceptor catalyst should increase n–σ* delocalization of the oxygen lone pair, rendering the α C–H bond more hydridic (more polarized) and more susceptible to HAT by an elecrophilic radical species.

We demonstrate the selective α-activation of alcohol C–H bonds in the presence of allylic, benzylic, α-oxy, and α-acyl C–H groups via a photoredox protocol, which relies on the cooperation of three distinct catalysts: an iridium-based photoredox catalyst; a HAT catalyst; and tetra-*n*-butylammonium phosphate (or TBAP), which is a hydrogen-bonding catalyst. On the basis of kinetic analyses, NMR structural data, and kinetic isotope effects (KIEs), we demonstrate the role of TBAP in facilitating the highly selective α hydrogen atom abstraction from alcohols.

The past several years have witnessed a dramatic increase in the application of photoredox catalysis—the use of visible light–activated organic dyes or metal complexes to facilitate single-electron transfer events—to the development of organic transformations (22). By combining photoredox activation with organocatalysis (23, 24) and nickel catalysis (25), we have recently highlighted the potential of photoredox catalysis to achieve bond constructions that are not possible with more traditional methods.

We became interested in the selectivity and efficiency of C–H bond activation in the context of our ongoing campaign to merge visible-light photoredox catalysis with HAT catalysis (26–29). We have previously demonstrated the utility of thiols (S–H BDE = 87 kcal/mol) as

HAT catalysts in the photoredox coupling of benzylic ethers (C–H BDE = 86 kcal/mol) with arenes (26) and imines (27). We recognized that the ability to catalytically activate stronger C–H bonds, such as those present in aliphatic alcohols and ethers (α C–H BDE > 90 kcal/mol), would hinge on the identification of a catalyst that satisfies two critical requirements: (i) homolytic cleavage of a strong substrate C–H bond must be counterbalanced by formation of a stronger H–[catalyst] bond, and (ii) selective activation of hydridic C–H bonds (bonds that are substantially polarized because of oxygen lone pair donation) must be realized. With these criteria in mind, we questioned whether it might be possible to transiently generate a hydridophilic amine radical cation from quinuclidine (Figs. 2A and 3)—which would be particularly suited to abstraction of relatively strong, hydridic C–H bonds—while resisting α-deprotonation because of poor H–C–N orbital overlap in this rigid bicyclic structure (30, 31). As outlined in Fig. 2A, we envisioned an initial excitation of the well-known photocatalyst $Ir[dF(CF_3)ppy]_2(dtbbpy)PF_6$ [$dF(CF_3)ppy$ = 2-(2,4-difluorophenyl)-5-(trifluoromethyl)pyridine, dtbbpy = 4,4’-di-*tert*-butyl-2,2’-bipyridine] (**1**) to $*Ir[dF(CF_3)ppy]_2(dtbbpy)^+$ (**2**) with visible light. Reductive quenching of **2** [reduction potential ($E_{1/2}^{red}$) = +1.21 V versus saturated calomel electrode (SCE) in $CH_3CN$] (32) via oxidation of **3** ($E_{1/2}^{ox}$ = +1.1 V versus SCE in $CH_3CN$) (33, 34) would then afford radical cation **4** and Ir(II) (**5**). At this stage, the electrophilic quinuclidinium radical **4** should abstract a hydrogen atom from an alcohol (**6**) to afford α-hydroxy radical **7** and quinuclidinium ion **8** [$H–N^+$ BDE = 100 kcal/mol (33)]. Nucleophilic addition of α-oxy radical **7** to an electron-deficient alkene would furnish alkyl radical **9**. Single-electron reduction of this electron-deficient radical **9** by Ir(II) (**5**) ($E_{1/2}^{red}$ = −1.37 V versus SCE in $CH_3CN$) would then afford the α-alkylated product **10** after protonation and lactonization, while simultaneously regenerating both the photocatalyst (**5**→**1**) and the HAT catalyst (**8**→**3**) (35, 36).

We initially validated our proposed alkylation protocol by subjecting 1-hexanol (**11**) and methyl acrylate to blue light in the presence of amine **3** [10 mole percent (mol %)] and photocatalyst **1**, which afforded after 24 hours γ-nonalactone (**12**) in 67% yield after acidic work-up (Fig. 2B). We next evaluated a range of hydrogen-bond acceptor catalysts, including the tetra-*n*-butylammonium salts of phosphate, trifluoroacetate, and diphenyl phosphate (Fig. 2B). Superior levels of product formation were achieved with catalytic TBAP (25 mol %), which provided the desired lactone in 84% yield. Initial rate kinetic analysis of the alkylation/lactonization of **11** revealed rate enhancements in the presence of each hydrogen-bonding catalyst examined, with the largest initial rate acceleration from use of $Bu_4NCO_2CF_3$ or $Bu_4N(PhO)_2PO_2$ [relative rate ($r_{rel}$) = 2.6 and 2.5, respectively].

We next demonstrated that a wide range of 1° and 2° alcohols undergo selective α-hydroxy alkylation with methyl acrylate in good to excellent yields using TBAP catalysis (Fig. 2C). As outlined in Fig. 3, these conditions clearly enable the selective activation of alcohol C–H bonds in the presence of various α-oxy C–H groups, including cyclic and acyclic alkyl ethers (**21**, **24**, and **25**, 85, 71, and 77% yield, respectively), silyl ethers (**23**, 73%yield), and esters (**22**, 81% yield). Moreover, excellent selectivity was achieved in the presence of both allylic and benzylic hydrogens (for example, **26** to **29**, 70 to 75% yield). The selectivity of this H-bond–assisted C–H activation platform was further demonstrated via the C–

Halkylation/lactonization of bifunctional steroid derivatives, which provided the corresponding lactone products in good levels of efficiency (**25** and **26**, 77 and 70%, respectively). Electron-deficient α-benzoyloxy and α-acyl C–H bonds (**22** and **26**) are expected to be inherently deactivated toward HAT with respect to electrophilic radical HAT systems (10), such as quinuclidinium radical cation. In the absence of TBAP, higher levels of substrate concentration were required to achieve useful efficiencies. However, under those conditions nonselective C–H abstraction of weaker, less hydridic C–H bonds was observed. In all cases outlined in Fig. 3, we only observed alkylation products arising from the activation of the hydroxyalkyl C–H bonds present in the various substrates.

We next turned our attention to defining the capacity for selective α-hydroxy C–H functionalization in the presence of C–H bonds that have similar polarity and strength. Specifically, we selected tetrahydrofuran (THF) as a prototypical ether substrate, which would normally undergo C–H activation via HAT with rates similar to those of alcohol substrates. We found that the dual catalytic system involving quinuclidine and photoredox catalyst **1** enabled the efficient alkylation of THF with rates that were competitive with 1-hexanol in competition experiments, affording a 1.7:1 mixture of lactone and ether products (Fig. 4A) (37). However, the addition of 25 mol % of TBAP catalyst enabled a dramatic increase in overall reaction selectivity to afford almost exclusively the alcohol C–H alkylation product (75% lactone, 1% ether).

To further understand the role of hydrogen bonding in this H-bond–assisted C-alkylation process, a series of computational calculations and NMR experiments were undertaken. These studies were to evaluate the interaction of 1-hexanol with various hydrogen-bonding catalysts (highlighted in Fig. 2B) and to determine their accompanying effect on the α-hydroxyC–H bond strength. We performed density functional theory (DFT) calculations using an unrestricted B3LYP functional with a 6–31G basis set. In the presence of either phosphate, diphenyl phosphate, or trifluoroacetate tetrabutylammonium salts, a BDE weakening of ~3 kcal/mol was calculated (supplementary materials). Although this represents a change in the α-C–HBDE of 1-hexanol from 94.1 kcal/mol to 91.0 kcal/mol when bonded to the TBAP catalyst, it clearly demonstrates that BDE is not the only factor defining this HAT selectivity, and bond polarization effects are likely important.

We also performed NMR experiments to explore the influence of both quinuclidine and TBAP as hydrogen-bonding catalysts for 1-hexanol. In the absence of either additive, the $^{13}C$ NMR chemical shift of the α carbon of 1-hexanol (δC1) in $CDCl_3$ (38) appeared at 63.1 parts per million (ppm) with $^{1}J_{CH[hexanol]}$ = 141.1 Hz. Addition of an equimolar amount of quinuclidine resulted in a 0.4-ppm upfield shift ($\delta C1_{hexanol:\mathbf{3}}$ = 62.7 ppm) and a slight decrease in the one-bond $^{13}C$–$^{1}H$ coupling constant ($^{1}J_{CH[hexanol:\mathbf{3}]}$ = 140.4 Hz). For comparison, a 1:1 mixture of 1-hexanol and TBAP gave rise to a similarly upfield shift in the $^{13}C$ signal for C1 of 1-hexanol ($\delta C1_{hexanol:TBAP}$ = 62.6 ppm; Δδ C1=0.5 ppm), with $^{1}J_{CH(hexanol:TBAP)}$ = 140.3Hz. These data clearly indicate that both quinuclidine and TBAP can induce bond weakening of the α-C1–H of 1-hexanol via hydrogen bonding. These data are also consistent with decreased *s*-character in the hybrid carbon orbitals of the C–H bond (increased hydridicity) of hexanol upon H-bond formation (39).

To more thoroughly outline the factors governing both the rate and selectivity of the C-alkylation of alcohols, we performed a suite of mechanistic experiments. The initial rate of the reaction of 1-hexanol with methyl acrylate showed first-order dependence on $[\text{hexanol}]_{\text{init}}$ and $[\text{acrylate}]_{\text{init}}$. The observed increase in the initial rate of reaction in the presence of TBAP (Fig. 2B), coupled with first-order dependence on both reactants, implies that TBAP serves to lower the energy barrier of (i) the C–H abstraction step (owing to α-C–H bond weakening); (ii) the C–C bond forming step, that is, addition of radical **9** to methyl acrylate (owing to enhanced nucleophilicity of the H-bonded α-hydroxy radical); or (iii) a combination of both of these steps.

In order to distinguish between these three possibilities, we conducted a series of experiments to assess potential deuterium kinetic isotope effects on the C–H abstraction step of the proposed catalytic cycle. First, the rate constants for the coupling of methyl acrylate with either 3-pentanol or D-3-pentanol (**30**→**16**) (Fig. 4B) were found to be identical—KIE = 1—clearly demonstrating that C–H/D abstraction from the alcohol **30** does not occur during the turnover-limiting transition state (TLTS) of our proposed catalytic cycle (Fig. 2A). However, an intramolecular competition experiment of monodeuterated alcohol **31** afforded a mixture of deuterated and undeuterated lactones ($P_D$ and $P_H$) with a 1.6:1 ratio (Fig. 4C). This result demonstrates that even though C–H/D abstraction is not rate-limiting, it represents the selectivity-determining step of the C-alkylation of hexanol **31**. The recovered starting material from this experiment did not contain any fully protonated 1-hexanol or $d_2$-hexanol, confirming that C–H/D abstraction is irreversible in this process. The irreversibility of the C–Habstraction step was further confirmed through two additional experiments: first, in an intermolecular competition between 1-hexanol and dideuterated hexanol **32** (Fig. 4D), in which no amount of monodeuterated alcohol **31** was detected during the process; and second, in the C-alkylation of enantiopure alcohol **33** (Fig. 4E), in which no racemization of starting material was observed upon recovery of excess starting material (40). Taken together, these results are consistent with the mechanistic scenario (iii): a dual role of TBAP in both accelerating the C–H abstraction from alcohols and enhancing the rate of addition of the resulting radical to Michael acceptors (41).

Last, compelling experimental evidence for our proposed C–H activation pathway was attained in the form of initial rate data for the conversion of cyclopropyl radical clock alcohol **35** to aldehyde **36** in the presence and absence of TBAP catalyst (Fig. 4F). Specifically, we reasoned that C–H abstraction from **35** to generate the 2-(alkoxycarbonyl) cyclopropylcarbinyl radical [rate constant for rearrangement = $5 \times 10^{10}$ to $8 \times 10^{10}$ $s^{-1}$ at 25°C (42–44)] would be rate-limiting. As such, enhancement in the rate of C–H abstraction via H-bond–assisted C–H activation should be clearly manifested in the observed rate of conversion of **35** to **36** in the presence and absence of TBAP catalyst. Indeed, under our photoredox/HAT conditions, a ninefold rate enhancement in the rate of conversion of alcohol **35** to aldehyde **36** was observed upon addition of 25 mol % TBAP (45). This result clearly corroborates our mechanistic proposal, in which TBAP facilitates C–H abstraction from alcohols via hydrogen bond activation. The activation concept presented here is likely pertinent to a wide range of C–H abstraction reactions.

## Supplementary Material

Refer to Web version on PubMed Central for supplementary material.

## ACKNOWLEDGMENTS

The authors are grateful for financial support provided by the NIH General Medical Sciences (R01 GM078201-05) and gifts from Merck and Amgen. J.L.J. is grateful for a NIH Postdoctoral Fellowship (F32GM109536-01), and J.A.T. thanks Bristol-Myers Squibb for a Graduate Fellowship.

## REFERENCES AND NOTES

1. Balcells D, Clot E, Eisenstein O. Chem. Rev. 2010; 110:749–823. [PubMed: 20067255]
2. Newhouse T, Baran PS. Angew. Chem. Int. Ed. 2011; 50:3362–3374.
3. Arndtsen BA, Bergman RG, Mobley TA, Peterson TH. Acc. Chem. Res. 1995; 28:154–162.
4. Lawrence JD, Takahashi M, Bae C, Hartwig JF. J. Am. Chem. Soc. 2004; 126:15334–15335. [PubMed: 15563132]
5. Chen MS, White MC. Science. 2010; 327:566–571. [PubMed: 20110502]
6. Mader EA, Davidson ER, Mayer JM. J. Am. Chem. Soc. 2007; 129:5153–5166. [PubMed: 17402735]
7. Warren JJ, Mayer JM. Proc. Natl. Acad. Sci. U.S.A. 2010; 107:5282–5287. [PubMed: 20215463]
8. Mayer JM. Acc. Chem. Res. 2011; 44:36–46. [PubMed: 20977224]
9. Paul V, Roberts BP. J. Chem. Soc. Chem. Commun. 1987; (17):1322.
10. Roberts BP. Chem. Soc. Rev. 1999; 28:25–35.
11. A Ti-catalyzed conjugate addition protocol enabled by complexation-induced N–H bond-weakening was recently reported (12).
12. Tarantino KT, Miller DC, Callon TA, Knowles RR. J. Am. Chem. Soc. 2015; 137:6440–6443. [PubMed: 25945955]
13. Bordwell FG, Harrelson JA Jr. Can. J. Chem. 1990; 68:1714–1718.
14. Blanksby SJ, Ellison GB. Acc. Chem. Res. 2003; 36:255–263. [PubMed: 12693923]
15. Laarhoven LJJ, Mulder P, Wayner DDM. Acc. Chem. Res. 1999; 32:342–349.
16. Steigerwald ML, Goddard WA III, Evans DA. J. Am. Chem. Soc. 1979; 101:1994–1997.
17. Evans DA, Baillargeon DJ. Tetrahedron Lett. 1978; 19:3315–3318.
18. Cradlebaugh JA, et al. Org. Biomol. Chem. 2004; 2:2083–2086. [PubMed: 15254636]
19. Gawlita E, et al. J. Am. Chem. Soc. 2000; 122:11660–11669.
20. Maiti NC, Zhu Y, Carmichael I, Serianni AS, Anderson VE. J. Org. Chem. 2006; 71:2878–2880. [PubMed: 16555846]
21. Pal U, Sen S, Maiti NC. J. Phys. Chem. A. 2014; 118:1024–1030. [PubMed: 24446840]
22. Prier CK, Rankic DA, MacMillan DWC. Chem. Rev. 2013; 113:5322–5363. [PubMed: 23509883]
23. Nicewicz DA, MacMillan DWC. Science. 2008; 322:77–80. [PubMed: 18772399]
24. Pirnot MT, Rankic DA, Martin DBC, MacMillan DWC. Science. 2013; 339:1593–1596. [PubMed: 23539600]
25. Zuo Z, et al. Science. 2014; 345:437–440. [PubMed: 24903563]
26. Qvortrup K, Rankic DA, MacMillan DWC. J. Am. Chem. Soc. 2014; 136:626–629. [PubMed: 24341523]
27. Hager D, MacMillan DWC. J. Am. Chem. Soc. 2014; 136:16986–16989. [PubMed: 25457231]
28. Jin J, MacMillan DWC. Angew. Chem. Int. Ed. 2015; 54:1565–1569.
29. Cuthbertson JD, MacMillan DWC. Nature. 2015; 519:74–77. [PubMed: 25739630]
30. The importance of polar effects in reactions of electrophilic radicals, such as aminium cation radicals, is well documented. An early example of selectivity in radical C–H functionalization is provided in (31).

31. Minisci F, Galli R, Galli A, Bernardi R. Tetrahedron Lett. 1967; 8:2207–2209.
32. Lowry MS, et al. Chem. Mater. 2005; 17:5712–5719.
33. Liu W-Z, Bordwell FG. J. Org. Chem. 1996; 61:4778–4783. [PubMed: 11667411]
34. Nelsen SF, Hintz PJ. J. Am. Chem. Soc. 1972; 94:7114–7117.
35. We cannot currently rule out the possibility that radical chain mechanisms are operative, in addition to the proposed closed catalytic cycle. A recent report on the characterization of radical chain processes in visible light photoredox reactions is provided in (36).
36. Cismesia MA, Yoon TP. Chem. Sci. 2015; 6:5426–5434.
37. In a related experiment using $d_8$-THF in place of THF, no deuterium exchange was observed between $d_8$-THF and 1-hexanol.
38. The propensity of $CD_3CN$ to form H-bonds with 1-hexanol precluded its use as a solvent for the measurement of changes in $^1J_{CH}$ as a function of H-bond formation with **3** or TBAP. However, small changes in δC1 were measured: $\delta C1_{hexanol}$ = 62.7 ppm, $\delta C1_{hexanol:\mathbf{3}\ (1:1)}$ = 62.6 ppm, and $\delta C1_{hexanol:TBAP\ (3:1)}$ = 62.6 ppm.
39. Balci, M. Basic $^1H$-$^{13}C$ NMR Spectroscopy. Amsterdam: Elsevier B. V.; 2005. p. 325-332.
40. For comparison, an intermolecular competition experiment between THF and $d_8$-THF gave rise to a 2:1 ratio of products, with the undeuterated ether as the major product.
41. A reaction coordinate diagram depiction of scenario (iii) is provided in the supplementary materials on *Science* Online.
42. Newcomb M, Choi SY. Tetrahedron Lett. 1993; 34:6363–6364.
43. Choi SY, Newcomb M. Tetrahedron. 1995; 51:657–664.
44. Newcomb M, Toy PH. Acc. Chem. Res. 2000; 33:449–455. [PubMed: 10913233]
45. As expected, when the same experiment was conducted in the presence of methyl acrylate (1 equivalent), none of the corresponding C–alkylation product was observed. Experimental details are provided in the supplementary materials on *Science* Online.

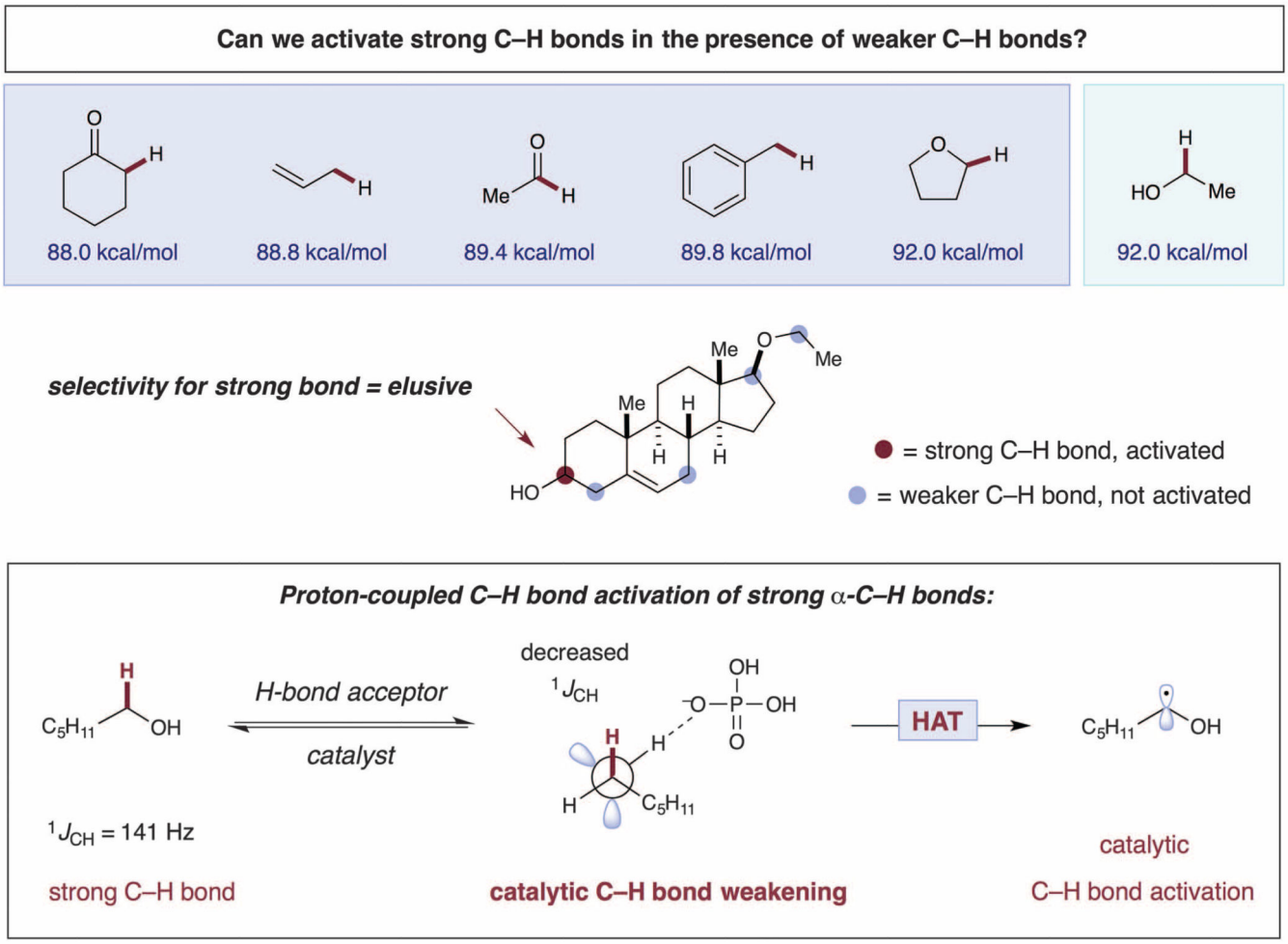


**Fig. 1. Proposed hydrogen bond–assisted C–H activation of alcohols**
BDE values are available in (13–15).

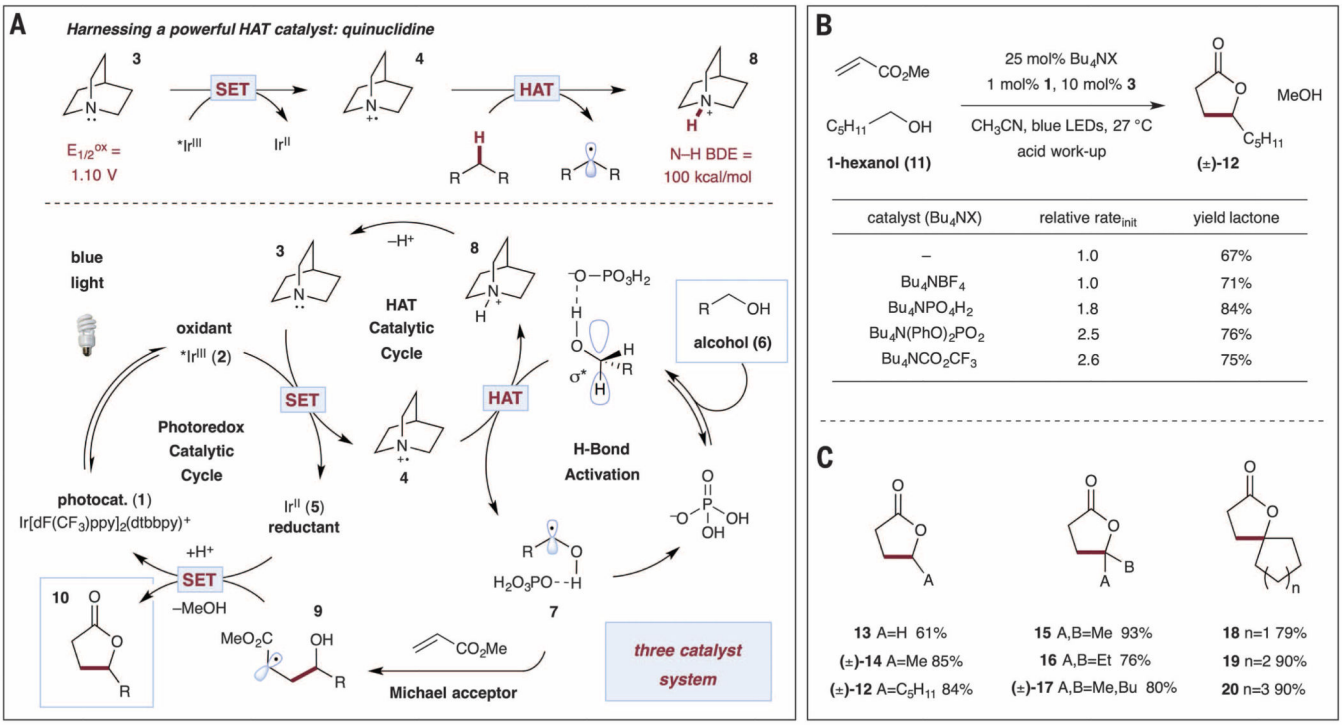


**Fig. 2. Reaction development**

(**A**) H-bond–assisted C–H activation of alcohols. Shown is a proposed mechanistic pathway for the C-alkylation of alcohols with Michael acceptors. SET, single-electron transfer. (**B**) Evaluation of hydrogen-bonding catalysts. Yield determined by means of $^{1}$H NMR, using an internal standard. (**C**) Selected scope of simple alcohol addition to methyl acrylate. Only products are shown; experimental conditions are as in (B). Isolated yields are reported.

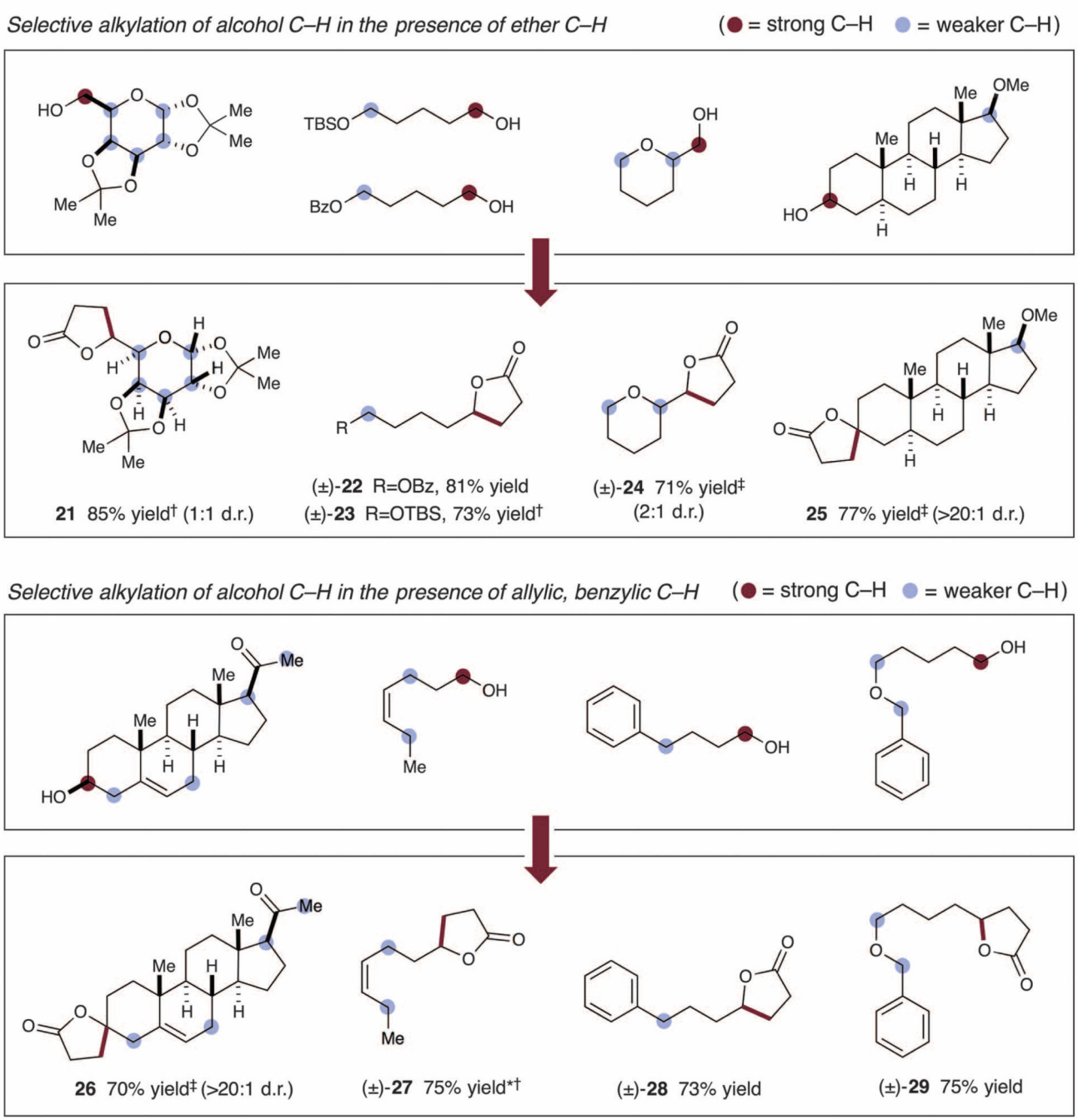


**Fig. 3. Selected alcohol scope for H-bond–assisted C–H activation**

Additions to methyl acrylate were carried out at 27°C for 24 hours, unless otherwise noted. Isolated yields are reported. Detailed experimental procedures and full scope of alcohols/Michael acceptors are provided in the supplementary materials. Dagger symbol indicates 40 hours reaction time; double-dagger symbol indicates 48 hours reaction time; and asterisk indicates 1:1 mixture of *E*/*Z* isomers. No alkylation of positions marked with blue circles was observed in any case.

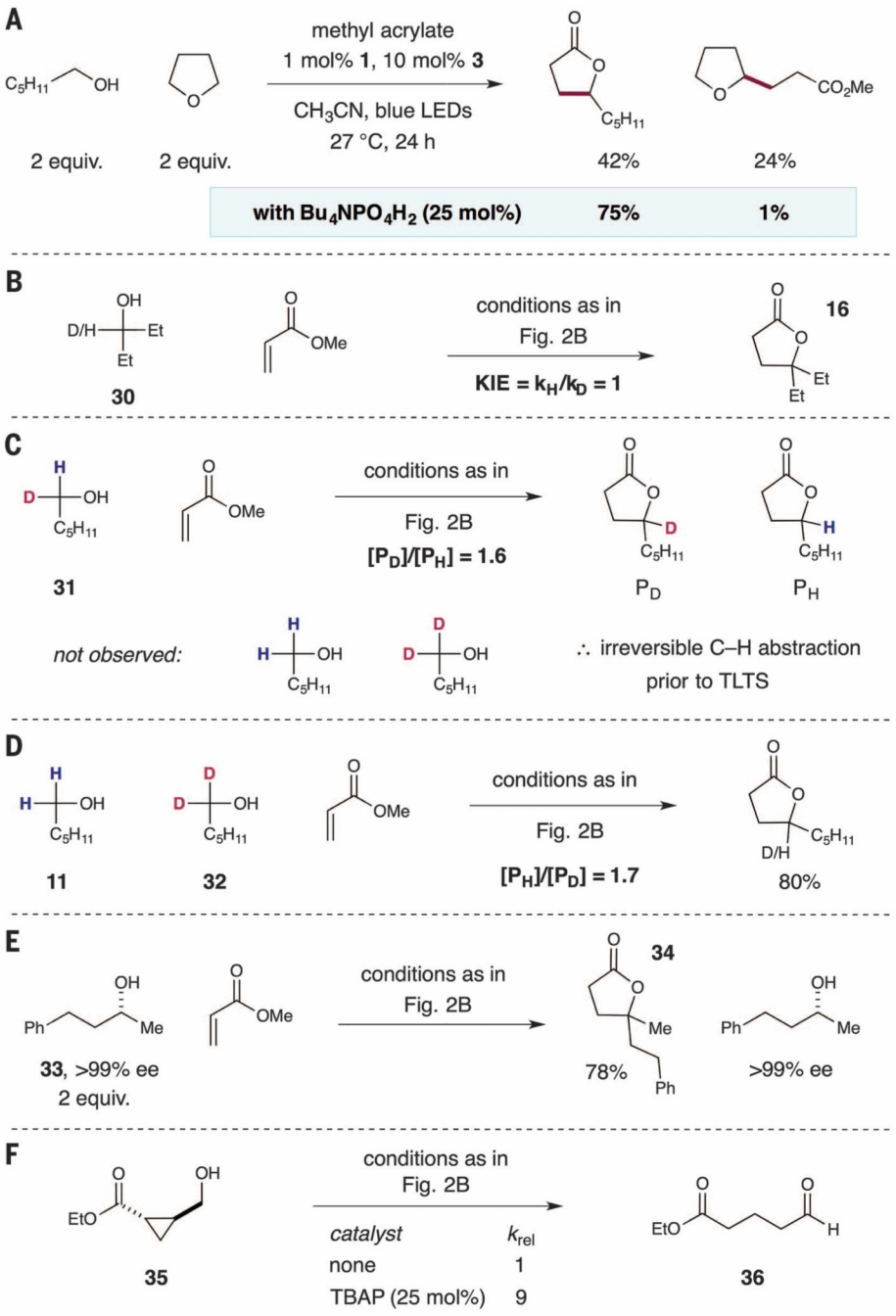


**Fig. 4. Mechanistic studies**

(**A**) H-bond–dependent selectivity of α-oxy C–H alkylation. (**B**) Kinetic isotope effect determined from two parallel kinetic analyses. (**C**) Kinetic isotope effect determined from intramolecular competition experiment. (**D**) Kinetic isotope effect determined from intermolecular competition experiment. (**E**) Evaluation of the enantiomeric excess of unreacted alcohol under standard C-alkylation conditions. (**F**) Effect of TBAP on the rate of C–H abstraction from **35**.